IEEE Access
Multidisciplinary | Rapid Review | Open Access Journal

Received March 2, 2021, accepted April 27, 2021, date of publication April 29, 2021, date of current version May 11, 2021.

Digital Object Identifier 10.1109/ACCESS.2021.3076670

Improving Distribution Networks' Consistency by Optimal Distribution System Reconfiguration and Distributed Generations

ABDULLAH M. SHAHEEN[1], RAGAB A. EL-SEHIEMY[2], (Senior Member, IEEE), SALAH KAMEL[3], EHAB E. ELATTAR[4], (Senior Member, IEEE), AND ABDALLAH M. ELSAYED[5]

[1]Electrical Engineering Department, Faculty of Engineering, Suez University, Suez 43533, Egypt
[2]Electrical Engineering Department, Faculty of Engineering, Kafrelsheikh University, Kafrelsheikh 33516, Egypt
[3]Electrical Engineering Department, Faculty of Engineering, Aswan University, Aswan 81528, Egypt
[4]Electrical Engineering Department, College of Engineering, Taif University, Taif 21944, Saudi Arabia
[5]Electrical Engineering Department, Faculty of Engineering, Damietta University, Damietta 34517, Egypt

Corresponding author: Abdallah M. Elsayed (am.elsherif@yahoo.com)

This work was supported by the Taif University Researchers Supporting Project, Taif University, Taif, Saudi Arabia, under Grant TURSP-2020/86.

ABSTRACT This paper presents an Enhanced Marine Predators Algorithm (EMPA) for simultaneous optimal distribution system reconfigurations (DSRs) and distributed generations (DGs) addition. The proposed EMPA recognizes the changes opportunity in environmental and climatic conditions. The EMPA handles a multi-objective model to minimize the power losses and enhance the voltage stability index (VSI) at different loading levels. The proposed EMPA is performed on IEEE 33-bus and large-scale 137-bus distribution systems (DSs) where three distinct loading conditions are beheld through light, nominal and heavy levels. For the 33-bus DS, the proposed EMPA successfully reduces the cumulative losses by 72.4% compared to 70.36% for MPA for the three-loading levels simultaneously. As a result, significant voltage improvement is achieved for heavy, nominal and light loadings to be 95.05, 97, 98.3%, respectively. For the 137-bus DS, it successfully minimizes the losses of 81.16% under small standard deviation 4.76%. Also, the 83-bus test system is considered for fair comparative between the proposed and previous techniques. The simulation outputs revealed significant improvements in the standard MPA and demonstrated the superiority and effectiveness of the proposed EMPA compared to other reported results by recent algorithms for DSRs associated with DGs integration.

INDEX TERMS Marine predators optimization, reconfiguration, distributed Generation, power losses, voltage stability.

NOMENCLATURE

ω_1 & ω_2	Weighting factors
N_{br}	Number of DS branches
N_n	Number of DS nodes
$Loss_{br}$	Active power losses in each branch (br)
VSI_n	Voltage stability index at node (n)
Lc	Each separate loading condition
N_{Lc}	Number of loading conditions
$TLoss_{Base}$	Basic loading without DSR and DG integration
O_T	Must open tie lines
No	Number of must open tie lines
Lg	Chosen nodes to install DGs
Pg	Output power from DGs
N_{dg}	Number of DGs
V_n	Voltage magnitude at each node (n)
I_{br} & I^{max}	Current flow in each branch and its thermal limit
Ps & Qs	Real and reactive power drawn from the substation
K_{PL}	DGs Penetration level
X^*	Updated position of each prey (i)
X_i	Current position for each prey (i)
R	Random uniformly distributed vector in [0, 1]
E	Elite matrix
R_m	Random variable describing Brownian motion

The associate editor coordinating the review of this manuscript and approving it for publication was Hui Ma.

E_i	Location of the top predator (i) in the Elite matrix.
It & Maxit	Current iteration and maximum number of iterations
P_S	Population size
Fit	Fitness function
R_n	Random vector dependent on the Lévy motion
XU & XL	Bounds of the control variables
FA	Probability vector of the fish aggregation
U	Regular binary array
E^*	Matrix of the current position for the top predator
X_{Bt}	Best position for the prey with the minimum fitness

I. INTRODUCTION

Power system experts are committed for improving the reliability of distribution networks. Planners and operators of distribution system aim at providing quantitative as well as qualitative power service and reducing the wasted energy in the electrical networks. This in turn not only enhances distribution systems (DSs) performance but also directly enhances the performance of transmission and generation systems as well as providing luxury and consumers' satisfaction [1]. Automating the DSs with DGs installation is considered one of the best followed solutions which can be implemented by optimal allocation and control of distribution system reconfigurations (DSRs), capacitor banks (CBs), distributed generators (DGs) and automatic voltage regulators (AVRs) in separate or combined manner [2], [3].

Radial topology of conventional DSs is an obstacle for achieving the benefits of DGs where excessive reverse power flow can be responsible of DGs shutdown and confront heavy economic burden in not exploiting these resources. Consequently, the planners and operators seek to optimally coordinate the DGs utilization with DSRs. DSRs is a process for optimally restructuring the distribution networks by altering the normally open switches (tie) and normally closed switches (sectionalize) within the distribution network. It also helps in enhancing DS reliability and DGs utilization [4].

The DSR problem has been firstly discussed by Merlin and Back [5]. In this study, a branch and bound algorithm has been employed to minimize the power loss. In [6], a modified simplex algorithm based-linear programming has been applied for the DSR problem for loss reduction, but it only acquired sub-optimal solution. Also, various analytical techniques have been applied which are usually based on distinct switching approaches such as close-all switch strategy [7]; sensitivities computation method [8]; Benders decomposition approach [9]. Otherwise, mixed integer programming (MIP) and meta-heuristic techniques are introduced for DSRs to overcome the shortages of the analytical methods. Ref [10] derives a set of linear current flow equations and then formulates the DSR problem for loss minimization as a MIP model. Optimal DSR based on a heuristic algorithm with developed convex relaxation of the AC optimal power flow is proposed for losses minimization [11]. The conventional algorithms have distinguished with fast convergence while the analytical techniques are simple and fast solution methods, but they lack the capability to treat multi-objective. Therefore, different artificial-based algorithms have been recently applied to DSR like Genetic algorithm (GA) [12], cuckoo search optimizer (CSO) [13], GA with varied population [14], backtracking search technique (BST) [15] and others.

In similar manner, several analytical methods were presented for optimal allocation of DGs. Modal analysis and continuous power flow were presented in [16] based on priority list formation. Exact loss formula was presented to find the optimal size and location of DG [17]. In this method, an analytical expression was presented where the load flow was required to be conducted only twice which declared less computation [18]. Artificial-based algorithms still present outstanding capability to maintain optimal solution accomplishment either for single or multi objectives [19]. Ref. [20] introduces a one rank CSO, which is formulated with multi-objectives of power loss minimization, voltage deviation minimization, and voltage stability improvement. Stochastic fractal search algorithm (SFSA) was introduced for minimizing the active power loss, improving the voltage profile, and increasing the voltage stability while satisfying various constraints [21] and others such as grey wolf optimizer [22], equilibrium algorithm (EO) [23]. In [24], GA has been applied for the optimum allocation of DGs and capacitor banks (CBs) in an economic cost estimation, but in this analysis, the number of DGs are pre-located on the basis of VSI prior to the optimization process. In [25], differential evolution (DE) algorithm has been utilized for the optimum allocation of multiple DGs. However, the economic cost calculation of this strategy has been overlooked. In [26], a hybrid algorithm based on outer and inner optimization stages have been presented to enhance the distribution sector. In this study, GA, particle swarm optimization (PSO) and exchange market algorithm (EMA) [27] have been combined for optimal allocation and scheduling of switched CBs in the distribution networks. In [28], EMA has been effectively applied in emergency conditions to optimally cluster the distribution sector into microgrids considering the presence of DGs and demand response programs.

Endeavors of DS operators and interested researchers have not ceased to achieve the best performance of DSs. One such endeavor is simultaneous control of DSRs and allocation of DGs. As such, recent studies to the implementation of an effective integration strategy has been presented; for example; manta ray foraging optimization [1]; harmony search algorithm (HSA) with an objective of minimizing real power loss and improving voltage profile [29]; combined GA and branch exchange [30]; artificial bee colony optimizer based on maximization of system loadability [31]; improved spotted hyena algorithm [32], improved elitist–jaya algorithm (IEJAYA) [5], FWA [33], firefly (FF) algorithm [34], sine-cosine algorithm [35], Harris Hawks

Optimizer (HHO) [36], invasive weed optimizer [37], salp swarm algorithm [38] and an improved beetle swarm optimization algorithm [39]. In [40], multi-objective particle swarm optimization (MOPSO) and non-dominated sorting genetic algorithm (NSGA-II) have been applied effectively for DGs allocation in distribution systems. In this study, the DGs penetration were maximized considering DSR. In [41], an advanced graphically based DSR has been introduced to minimize the power losses. Despite its applicability to large DSs, near-optimal solutions for the DNR issue might be obtained. In [42], recent Archimedes optimizer has been utilized for DG planning algorithm considering the DSR and soft open points. In [43], sunflower algorithm has been carried out to reallocate the capacitors in distribution systems considering DSR problem and handling DGs of wind type via Monte-Carlo simulation. In [44], DSR were utilized by DigSilent PowerFactory program to improve the reliability of a practical case study. In [45], the allocation of distributed generation units is carried out considering the distribution system configuration. The mix objective aims at minimizing the planning costs among certain studied area. The application is limited to small system only. The solver GUROBI was used the considered problem. In [46], the mixed problem of DGs allocation and network configuration is solved by a methodology based on learning automata. The distribution of energy storage system for reconfigurable distribution system is considered in [47]. In [48], a bi-stage procedure was presented for managing the energy for hybrid AC/DC systems through multi-objective framework. Two objectives are considered as minimization of operation costs and power losses. In [3], [49], the network reconfiguration is coordinated with DGs and voltage regulators. The mix allocation problem of DGs and reconfiguration network was developed for unbalanced systems in [49] and [50]. In [51], the enhanced Disturbed Beetle Antennae with Chaos Search was employed for solving Multiobjective Reconfiguration problem taking into account the variation of Loading level and DGs types. Reference [52] presented a study on the radiality limitations for distribution systems that are restored after faults where the reconfiguration process is necessary. The impact of reconfiguration process on the protection system was discussed on [53].

As seen above, few recent literatures handle simultaneous distribution reconfiguration with DGs. Also, practical load variation is not satisfactory covered in literatures which simulate practical load pattern in different days and seasons. Otherwise, multi-objective achievement of such problem is another challenge that many techniques may fail to accomplish in such a case and make it difficult to achieve the optimal solution. The EMPA is proposed for simultaneous optimal DSRs and DGs integration. It is developed to reduce overall power losses and maximize voltage stability as a multi-objective model while preserving both technical and operational constraints considering practical load variations. The developed EMPA have high superiority and more effectiveness compared with several optimization techniques to obtain realistic solutions for IEEE 33 bus. The validity of the proposed EMPA is assessed for large-scale 137-bus DSs. Also, the 83-bus test system is considered for fair comparative between the proposed and previous techniques literature.

The remainder of the paper is structured as follows. In section II, the formulation of the problem is presented along with the different restrictions considered in the proposed model. Section III focuses on the proposed EMPA and its employment. Results are discussed in Section IV whilst section V derives the conclusions of the study.

II. PROBLEM FORMULATION

The DSR and DGs integration aims to minimize the losses in the DS branches and maximize the overall VSI. Both objectives can be incorporated as follows:

$$O_1 = \text{Min}\left\{(\omega_1 \sum_{br=1}^{N_{br}} \text{Loss}_{br}) + (\omega_2 \frac{1}{\sum_{n=1}^{N_n} \text{VSI}_n})\right\} \quad (1)$$

The VSI ranges from zero at the voltage failure point to unity at no load and can be simply calculated as in (2).

$$\begin{aligned}\text{VSI}_n = {} & V_{n-1}^4 - 4(P_{n,\text{eff}}X_{n-1} - Q_{n,\text{eff}}R_{n-1})^2 \\ & - 4(P_{n,\text{eff}}X_{n-1} - Q_{n,\text{eff}}R_{n-1})V_{n-1}^2, \quad n = 2, \ldots N_n\end{aligned} \quad (2)$$

Despite this objective model have been investigated in several applications [29], [33]–[35], Therefore, the weighted sum approach is estimated to normalize the two objectives [54]. Analysis of a specified loading may cause excessively-sizing problems [55] since it ignores the realistic existence of the daily load differences. As a result, multiple loadings can be assisted, and the target goal can be updated as:

$$O_2 = \text{Min} \sum_{Lc=1}^{N_{Lc}} \left\{(\omega_1 \frac{\sum_{br=1}^{N_{br}} \text{Loss}_{br}}{\text{TLoss}_{\text{Base}}}) + (\omega_2 \frac{N_n}{\sum_{n=1}^{N_n} \text{VSI}_n})\right\}_{Lc} \quad (3)$$

This model looks for the appropriate location of the open lines for reconfiguration purposes, and the optimal position and scale of DGs. The position of DGs is set no matter how sophisticated the loading is. On the opposite, DGs outputs are dispersed to optimize the gains. Therefore, the control variables vector (V_C) is as shown at the bottom of this page.

$$V_C = \{\underbrace{[O_{T1}\ O_{T2} \ldots\ldots O_{TNo}]}_{\text{Open Tie lines}};\ \underbrace{[Lg_1\ Lg_2 \ldots\ldots Lg_{N_{dg}}]}_{\text{DG Locations}};\ \underbrace{[Pg_{1,1} \ldots\ldots Pg_{N_{dg},1}, Pg_{1,2} \ldots\ldots Pg_{N_{dg},2}, \ldots Pg_{1,Lc} \ldots Pg_{N_{dg},Lc}]}_{\text{Output power of DGs for each loading condition}}\} \quad (4)$$

O_T, No, N_{dg} and Lg must take an integer number whereas Pg is varied in a continuous manner with the loading. In addition, several constraints must be maintained as follow:

$$V_{k,Lc}^{min} \le V_{k,Lc} \le V_{k,Lc}^{max} \quad Lc = 1 \ldots N_{Lc},\ k = 1, \ldots . N_n \tag{5}$$

$$\left|I_{br,Lc}\right| \le I_{br,Lc}^{max} \quad br = 1 \ldots . N_{br},\ Lc = 1 \ldots N_{Lc} \tag{6}$$

$$1 \le O_{T-m} \le No \quad m = 1 \ldots \ldots . No \tag{7}$$

$$1 \le Lg_k \le N_n \quad k = 1 \ldots \ldots . N_n \tag{8}$$

$$0 \le Pg_{k,Lc} \le Pg^{max} \quad Lc = 1 \ldots . . N_{Lc},\ k = 1 \ldots . . N_n \tag{9}$$

$$\left\{\sum_{j=1}^{N_{Dg}} Pg_j\right\}_{Lc} \le K_{PL}\left\{\sum_{n=1}^{N_n}(Qd_n)\right\}_{Lc} \quad Lc = 1, 2, \ldots \ldots . N_{Lc} \tag{10}$$

$$(Ps + \sum_{j=1}^{N_{Dg}} Pg_j)_{Lc} > \sum_{n=1}^{N_n}(Pd_n)_{Lc}, \quad Lc = 1, 2, \ldots \ldots . N_{Lc} \tag{11}$$

$$Qs_{Lc} > \sum_{k=1}^{N_n}(Qd_k)_{Lc}, \quad Lc = 1 \ldots . . N_{Lc} \tag{12}$$

The subscripts ''min'' and ''max'' indicates the minimum and maximum of each variable. As shown, the voltage quality at each node of the DS for all loading levels is kept within its permissible bounds as inequality constraints as in (5). In addition, the inequality bounds of the Ampere flow that is passed through each branch and loading is maintained in (6). Eq. (7) represents the inequality constraints related to the tie lines since there is meaningless to select lines to be open less than 1 or more than their cumulative number. Similarly, (8) represents the inequality constraints related to the candidate DG locations within the total number of the DS nodes. Also, (9) represents the inequality constraints related to the outputs of the DGs not to be more than the specified sizes. Eq. (10) presents a constraint to assure that the summation of the generated power from the DGs at any loading level is within the acceptable penetration level specified by 'K_{PL}' which is taken 60% [29]. Eqs. (11) and (12) ensure powering all the distribution nodes where the supplied real and reactive power from DGs and substation must be more than the total load. Nevertheless, the radial configuration of the DS is maintained in operation where a branch-bus incidence matrix is composed by the following expression:

$$A_{ij} = \begin{cases} 0, & \text{if line i isn't connected to bus j} \\ -1, & \text{if the line i enter to bus j} \\ 1, & \text{if the line i exits from bus j} \end{cases} \tag{13}$$

This matrix is $N_n \times N_{br}$. The DS configuration can be judged as radial form if their determinant is 1 or -1 whilst the DS is not in radial form if it is zero [15].

III. EMPA FOR OPTIMAL CONSISTENCY PROCEDURE

A. ENHANCED MARINE PREDATORS ALGORITHM

Marine Predators Algorithm (MPA) is a new algorithm of optimization that is inspired by nature by the diverse techniques followed by predators to maximize their prey hunting rates [56]. These tactics are based on Lévy and Brownian campaigns, which are increasingly encouraged by the environment, and predators eventually follow strategies for survival. The MPA starts with a uniform distribution and random initialization of the locations of the prey where their number reflects the size of the population. The fittest solution is then created and rated as the top predator, which is copied into the Elite matrix (E) with same size as the population.

In MPA, the searching process to capture the prey passes through three sequential stages, such that iterations are separated into three distinct and consecutive sections. In the first phase of the search, predators are in the process of being detected by military observation of the surrounding environment. In the second step of the search, predators may choose the suitable prey, or may still be finding the target. This scenario is being done in the midst of the MPA iterations. In the last MPA phase of the iterations, the predator is in the act of stalking, so that it moves quicker than the victim. This example reflects the potential of predators to manipulate their intended prey. In certain cases, the prey is lost on the way to predators, or other predators are cleverer in hiding and destroying their victims. The separation of the iterations into three distinct and sequential sections cancels the probability of the existence of these circumstances. The EMPA is then established that the EMPA proposes to provide a random probability of combining these measures and therefore the updating mechanism of the new positions of the preys is mathematically represented as in (Eq. 14). In Eq. (16), C_{It} is a

$$\vec{X_i}^* = \begin{cases} \vec{X_i} + 0.5\vec{R} \otimes \vec{R_m} \otimes (\vec{E_i} - \vec{R_m} \otimes \vec{X}_i) & \text{if } It \le \dfrac{Maxit}{3} \,\&\, \text{if rand} \le \text{rand} \\ \vec{X_i} + 0.5\vec{R} \otimes \vec{R_n} \otimes (\vec{E_i} - \vec{R_n} \otimes \vec{X_i}) & \text{if } \dfrac{Maxit}{3} < It \le \dfrac{2Maxit}{3} \,\&\, \text{if } i \le \dfrac{P_S}{2} \,\&\, \text{if rand} \le \text{rand} \\ \vec{E_i} + 0.5C_{It} \otimes \vec{R_m} \otimes (\vec{R}_m \otimes \vec{E_i} - \vec{X}_i) & \text{if } \dfrac{Maxit}{3} < It \le \dfrac{2Maxit}{3} \,\&\, \text{if } i > \dfrac{P_S}{2} \,\&\, \text{if rand} \le \text{rand} \\ \vec{E_i} + 0.5C_{It} \otimes \vec{R_n} \otimes (\vec{R}_n \otimes \vec{E_i} - \vec{X}_i) & \text{if } It \ge \dfrac{2Maxit}{3} \end{cases} \tag{14}$$

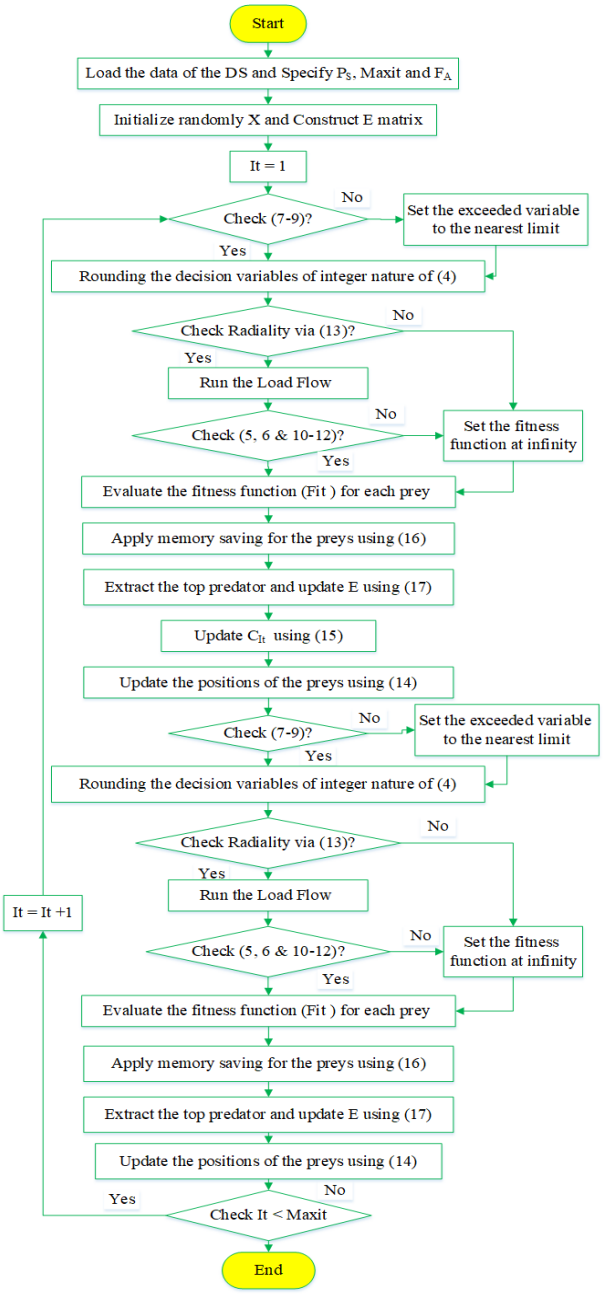

FIGURE 1. Flow chart of the EMPA for optimal DSRs and DGs integration.

parameter that is adaptively varied with iteration development to monitor the predator locomotion. It is formulated as in Eq. (15).

$$C_{It} = (1 - \frac{It}{Maxit})^{(\frac{2It}{Maxit})} \tag{15}$$

After this update program, if the locations of the prey have been changed, the fitness (Fit) of each prey is measured and the memory of the marine predators is executed as in (16).

$$\vec{X}_{i,It+1} = \begin{cases} \vec{X_i}^* & \text{if Fit } (\vec{X_i}^*) \le \text{Fit } (\vec{X_i}) \\ \vec{X_i} & \text{if Fit } (\vec{X_i}^*) > \text{Fit } (\vec{X_i}) \end{cases} \tag{16}$$

Also, the enhancement plan for the top predator is carried out by matching the fitness of the Leader with the optimal health of the prey as in (17).

$$\vec{E_i}^* = \begin{cases} \vec{X}_{Bt} & \text{if Fit } (\vec{X}_{Bt}) \le \text{Fit } (\vec{E_i}) \\ \vec{E_i} & \text{if Fit } (\vec{E_i}) \le \text{Fit } (\vec{X}_{Bt}) \end{cases} \tag{17}$$

In addition to the adjustment of the locations of the prey in (16), the environmental effects of the Fish Aggregation (FA) have been endorsed. Marine predators can also take longer leaps in unruly dimensions to check for prey concentrations in the aquatic area. In the other hand, the presence of fish aggregations can cause local optimum trapping problems.

$$\vec{X_i}^* = \begin{cases} \vec{X_i} + C_{It}(\vec{X_L} + \vec{R} \otimes (\vec{X_U} - \vec{X_L}) \otimes \vec{U} & \text{if } r_1 \le F_A \\ \vec{X_i} + (\vec{X_x} - \vec{X_y}).(F_A(1 - r_1) + r_1) & \text{else} \end{cases} \tag{18}$$

B. PROPOSED EMPA FOR OPTIMAL DSRS AND DGS INTEGRATION

The EMPA is described for optimal DSRs and DGs integration in the flow chart of Fig. 1. This figure presents several issues to resolve the considered formulation as:-

- Integer code is presented for the open tie sections and the DGs positions. The DGs outputs respective to every loading stage are represented in continuous manner.
- Eqs. (7-9), that represents the constraints of the decision variables, are self-maintained in the EMPA.
- The limits in (5, 6, 10-12) are not self-bounded so the considered fitness will set to infinity if there is any break in someone of these constraints after performing the power flow.
- Verification of the radial topology of the DS is carried out by (13) until the power flow begins.

IV. APPLICATIONS

Several applications are executed based on the MPA and the proposed EMPA on the IEEE 33-bus and large scale 137-bus DSs. Also, the 83-bus test system is considered for fair assessment between the presented EMPA and other methods.

Two different cases are based on the handled objective. ***Case 1***, minimization of the power losses is considered as single objective function. So, the weight factors ω_1 and ω_2 in (3) are set to 1 and 0, respectively. ***Case 2***, both objectives are considered as in (3) where the weights ω_1 and ω_2 are taken 70 and 30 %, accordingly [20]. The two cases are conducted concurrently at three loading conditions of 0.5 (light), 1.0 (nominal), 1.6 (heavy). The parameters used for each EMPA are Maxit = 200, P_S = 50, number of runs = 10. The value of the voltage of the node should be limited to ±5 percent of the measured voltage. The maximum number of three DGs can be mounted. The capability of each DG is limited to 3 MW.

A. OPTIMAL DSR AND DGS INTEGRATION FOR THE 33-BUS DS

The first DS is the IEEE 33-bus which its initial configuration is displayed in Fig. 2. As shown, it has 32 sectional lines (numbered from 1 to 32) and 5 open lines (numbered from 33 to 37) [32]. For the nominal loading, the overall real, reactive, and apparent power requirement are 3.715 MW, 2.3 MVAR and 4.369 MVA, respectively.

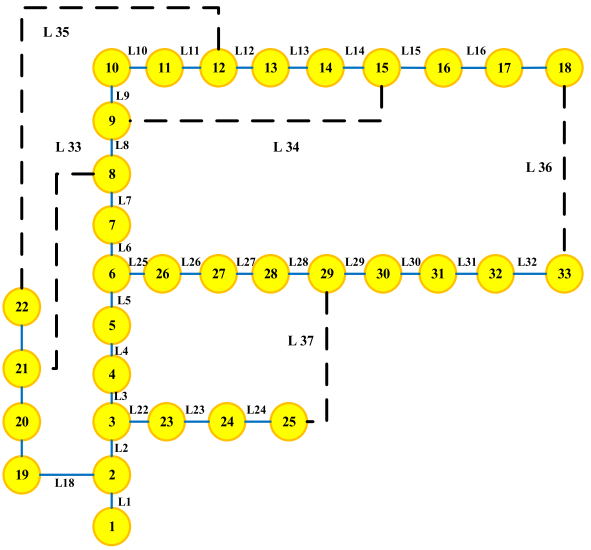

FIGURE 2. IEEE 33-bus power DS.

1) EMPA APPLICATION CONSIDERING THREE LOADING CONDITIONS SIMULTANEOUSLY FOR CASE 1

In that case, the proposed EMPA and the MPA are applied for the minimization of the power losses (10) as a single objective function. At the same time, the three loading conditions of 0.5 (light), 1.0 (nominal), 1.6 (heavy) are handled simultaneously. For Case 1, both MPA and EMPA are applied for optimal DSR and DGs integration for 10 times and their best results are staggered in Table 1.

TABLE 1. MPA and EMPA results of the 33-bus DS for Case 1 considering distinct loading conditions.

		Base	MPA			Proposed EMPA		
Open lines		33-37	7, 14, 28, 35 and 36			8, 9, 28, 33 and 36		
Installed buses of DGs			12	15	30	8	29	33
DGs Outputs (kW)	Light	-	351	200	561	853	101	144
	Nominal		181	748	1300	562	984	683
	Heavy		594	829	2143	879	1594	1093
kW Losses	Light	47.067	14.39			18.82		
	Nominal	202.66	64.16			57.2		
	Heavy	575.31	165.91			151.28		
Sum (kW Losses)		825.04	244.47			227.3		

From this table, the proposed EMPA selects the lines 8, 9, 28, 33 and 36 to be in open state while all the others are in closed state. It also specifies three nodes of 8, 29 and 33 to install DGs and their outputs are optimally varied with the load variations. At the light loading, the outputs are 853, 101, and 144 kW for the DGs at nodes 8, 29 and 33, respectively. They are varied to 562, 984, and 683 kW, and 879, 1594, and 1093 kW at nominal and heavy loadings, respectively. It is observed that the power losses by using the suggested EMPA are reduced by 60, 71.8 and 72.4% for light, nominal and heavy loading, respectively, and a cumulative loss reduction of 72.4% for the three-loading process at the same time.

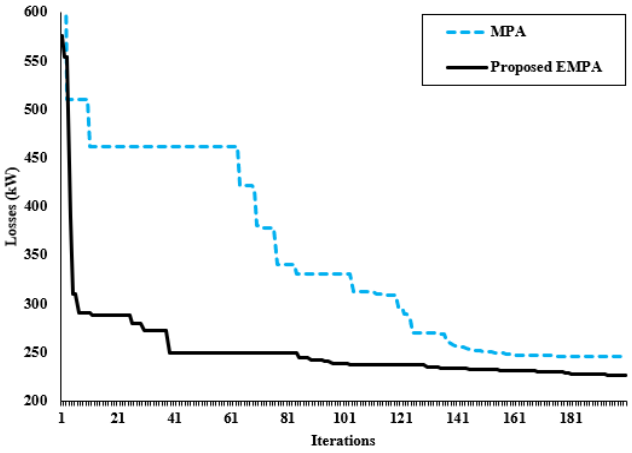

FIGURE 3. Convergence characteristics of MPA and EMPA for Case 1 of the 33-bus DS.

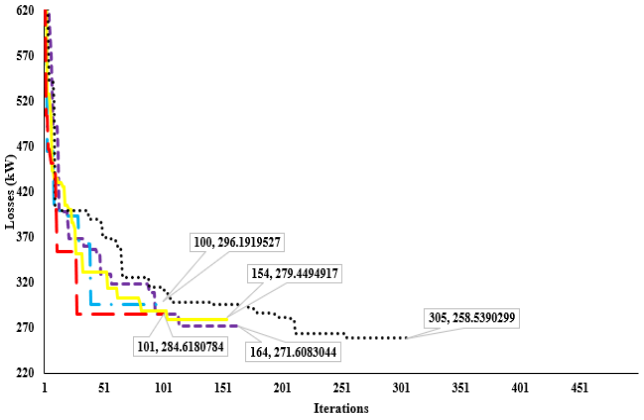

FIGURE 4. MPA convergence rates with adaptive stop criterion for Case 1.

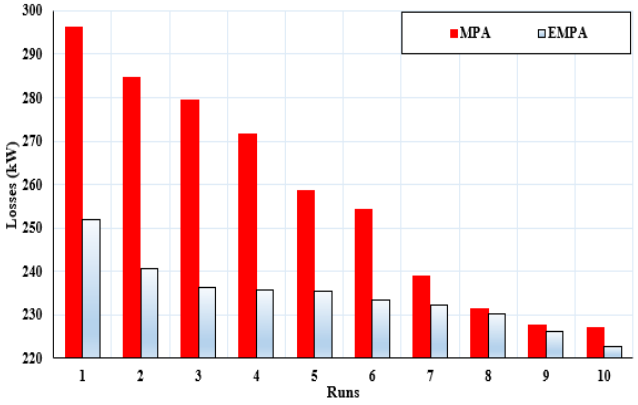

FIGURE 5. Cumulative kW losses for the 10 runs with adaptive stop criterion for Case 1.

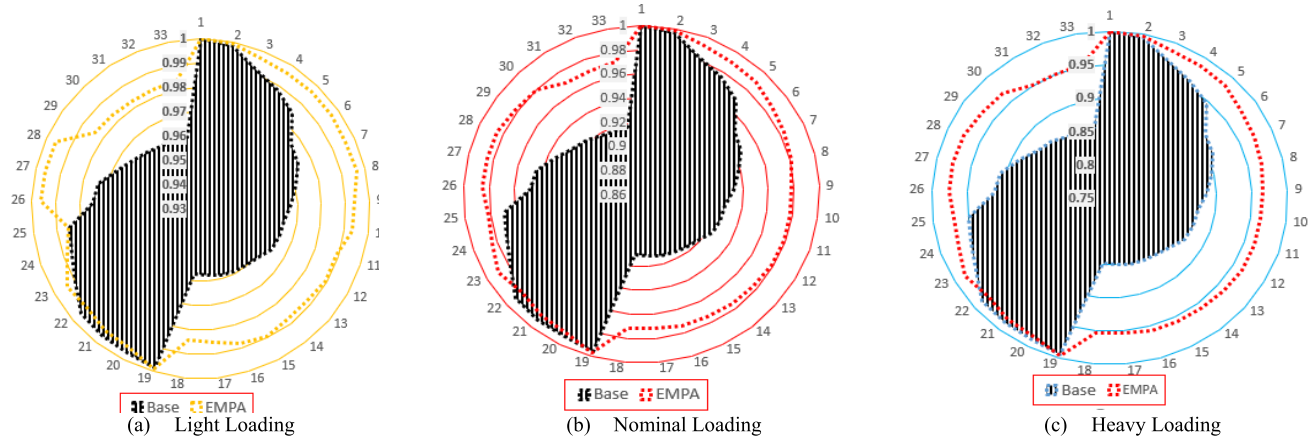

(a) Light Loading (b) Nominal Loading (c) Heavy Loading

FIGURE 6. Nodes voltage of the 33-node system for multiple load conditions of Case 1.

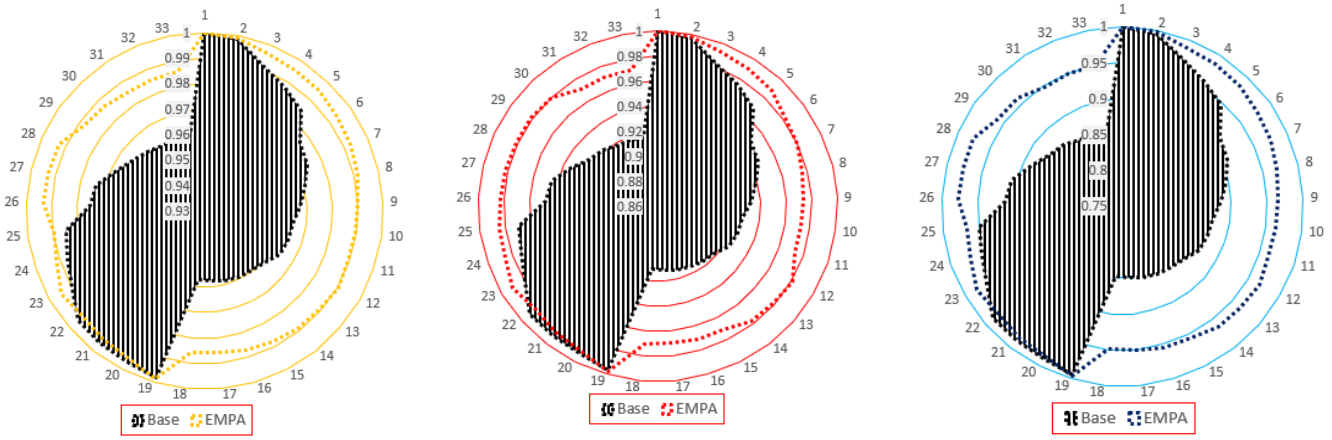

(a) Light Loading (b) Nominal Loading (c) Heavy Loading

FIGURE 7. Nodes voltage of the 33-node system for multiple load conditions of Case 2.

TABLE 2. Statistical values for MPA and EMPA with adaptive stop criterion of the 33-bus DS for Case 1.

	MPA	EMPA
Infeasible problem variables exceeding the minimum	7 %	6.13 %
Infeasible problem variables exceeding the maximum	21.38 %	8.24 %
Total infeasible problem variables	28.35 %	14.36 %
Updated solutions replicating old solutions	23.155 %	51.78 %
Solutions replicating the global best	28.74 %	37.68 %

TABLE 3. MPA and EMPA results of the 33-bus DS for multiple load conditions of Case 2.

		Base	MPA			Proposed EMPA		
Open lines		33-37	7, 8, 34, 36 and 37			11, 14, 28, 30 and 33		
Installed DG buses			14	25	30	8	25	32
DGs Outputs (kW)	Light	-	409	123	579	406	392	316
	Nominal		385	963	881	200	1223	806
	Heavy		1249	628	1689	1224	1363	979
kW Losses	Light	47.067	15.95			13.78		
	Nominal	202.66	66.38			60.17		
	Heavy	575.31	165.66			148.29		
TVSI	Light	28.84	30.06			28.98		
	Nominal	25.77	28.4			27.83		
	Heavy	22.22	27.79			26.64		
Fitness		-	1.47			1.42		

On the other side, traditional MPA reduces the losses by 69.4, 68.3 and 71.2%, respectively for light, nominal and heavy loading and decreases the overall losses by 70.4% for the three-loadings at the same time. Fig. 3 depicts the characteristic of convergence for MPA and EMPA which shows the success of the changes adopted by the EMPA to achieve the near global optimum solutions. As seen in Fig. 3, the EMPA has good convergence rates compared with MPA.

Another point for comparative concerns, an adaptive stop criterion is activated, as reported in [48], by specifying a very high value of 500 for the maximum number of iterations and applying a stop capability when no improvement is occurred in the last K iterations. K is a user-defined that is taken 50. Ten runs are performed for both MPA and EMPA. It is noticed that 50% of the total runs of the standard MPA is stopped before reaching the 500 iterations. Fig. 4 illustrates samples of the MPA convergence rates which are prematurely stopped at the iteration 100, 101, 154, 164, and 305. On the other side,

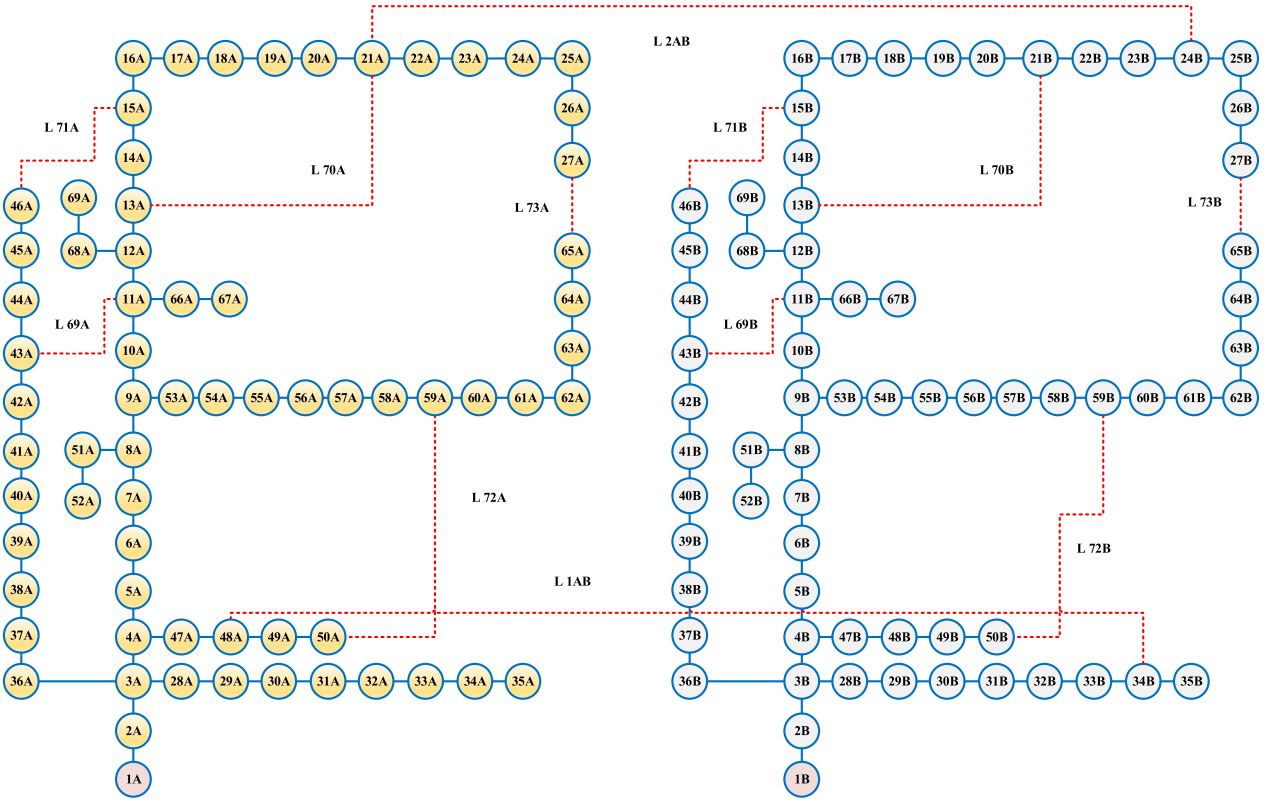

FIGURE 8. The 137-bus large-scale DS.

TABLE 4. Different versus equal weights based on the EMPA.

	Different weights		Equal weights		Increase Percentage
	ω_1 =70	ω_2 = 30 %	ω_1 = 50 %	ω_2 = 50 %	
Sum (Losses)	222.24		236.5717		6.05 %
Sum (OVSI)	83.45		86.8417		3.905 %

TABLE 5. Robustness indices of MPA and EMPA for Cases 1 and 2 for the 33-bus DS.

Indices	Case 1		Case 2	
	MPA	EMPA	MPA	EMPA
Best	246.4780152	227.3040589	1.467798993	1.419823401
Medium	278.3145047	237.8156328	1.572481249	1.463265788
Worst	318.9352358	248.1833404	1.678941738	1.508461829
Std	24.05976078	6.809622977	0.087972247	0.030512914

the proposed EMPA takes the maximum number of iterations without premature stopping. Fig. 5 displays the cumulative kW losses, in a descending order, for the runs considering adaptive stop criterion. As shown, the proposed EMPA is superior to MPA with best of 222.72, medium of 234.5 and worst of 251.9 compared to 227.02, 257 and 296.2, for the MPA, respectively.

Added to that, the average percentage of the infeasible problem variables, updated solutions replicating old solutions, and solutions replicating the global best are estimated and tabulated in Table 2. This table shows the higher ability of the proposed EMPA in reducing the infeasible variables during the iterations since it reports nearly half number of the infeasible variables of the MPA.

TABLE 6. MPA and EMPA applications for the 33-bus DS.

Loading	Items	Base	MPA	Proposed EMPA
Light	Open lines	33-37	8, 13, 28, 33, 36	10,2 8, 33, 34, 36
	DGs buses (kW)	--	239(7), 234(15), 641(29)	253(7), 229(15), 632(29)
	kW Losses	47.067	14.667	14.471
Nominal	Open lines	33-37	10, 14, 28, 32, 33	7, 8, 10, 28, 32
	DGs buses (kW)	--	722(9), 66(27), 1391(29)	814(15), 1415(29)
	kW Losses	202.66	63.0889	61.257
Heavy	Open lines	33-37	8, 28, 33, 34, 36	7, 12, 28, 32, 35
	DGs buses (kW)	--	1185(7), 746(15), 1635(30)	687(9), 794(16), 2085(30)
	kW Losses	575.31	161.278	160.937

In comparison, the updated solutions that replicate the old ones based on the EMPA with a percentage of 51.78% are more than the double percentage gained by the MPA of 23.155%. Not just that, but even the solutions that replicates the global best via EMPA with a percentage of 37.68% are better than the 28.74% of MPA solution. These statistical values reflect the substantial change that has arisen in the MPA using the proposed EMPA. Fig. 6 displays the voltage profile over all the DS nodes for light, nominal and heavy loadings. As shown, it is evident that a sufficient improvement in voltage can be obtained by applying the proposed EMPA for all loading conditions where the minimum voltages are 0.9505, 0.970, 0.9829 p.u for heavy, nominal and light loadings, respectively after applying the proposed EMPA, while the minimum voltages for the base case are 0.9571, 0.9105 and 0.8481, respectively.

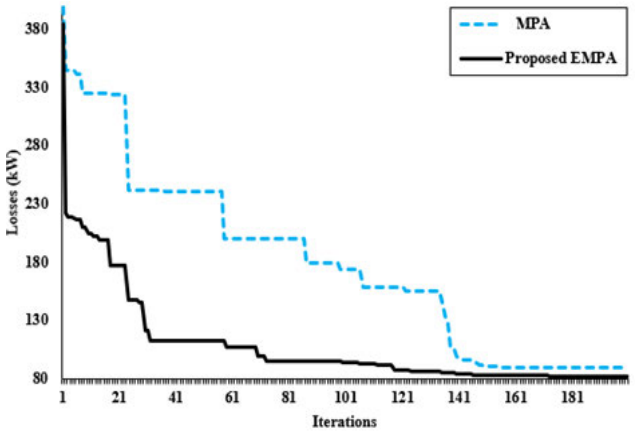

FIGURE 9. Convergence rates of the EMPA and MPA at for 137-bus DS.

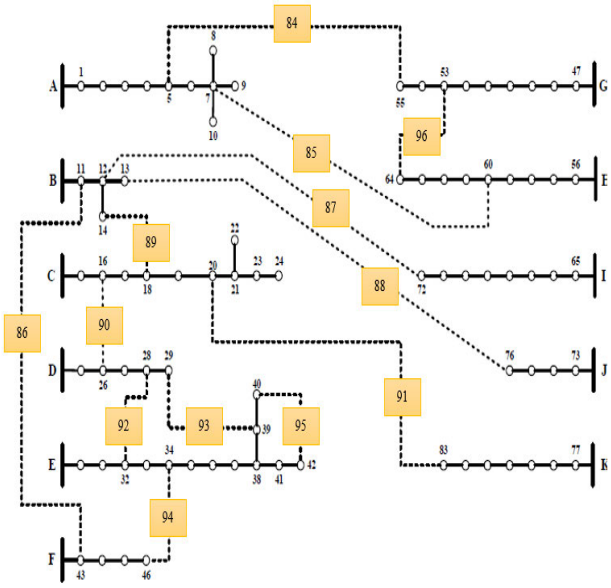

FIGURE 10. The 83-bus DS.

2) EMPA APPLICATION CONSIDERING THREE LOADING CONDITIONS SIMULTANEOUSLY FOR CASE 2

In that case, the proposed EMPA and the MPA are applied for multi-objective losses minimization and VSI improvement. At the same time, loading conditions of 0.5 (light), 1.0 (nominal), 1.6 (heavy) are handled. Analogous to case 1, an optimal joint DSR and DGs integration can be accomplished by the proposed EMPA. For this case, it is used to accomplish losses minimization and VSI improvement objective functions. Table 3 displays the obtained decision variables and the targets for the MPA and the new EMPA. Power losses are lowered by 70.7 percent, 70.3 percent and 74.2 percent, respectively.

On the other side, standard MPA will minimize power losses by 66.1%, 67.2% and 71.2% respectively for light, nominal and heavy loads. The proposed EMPA and standard MPO will efficiently improve the voltage stability of the delivery system by increasing the overall VSI to 28.97, 27.82 and 26.63 for light, nominal and heavy loads, respectively, using the proposed EMPA and to 30.06, 28.40 and 27.78, respectively, for light, nominal and heavy loading by using the MPA. Fig. 7 shows the voltage profile over all the DS nodes for light, nominal and heavy loadings for base case and after optimal DSR and DG integration via the proposed EMPA which completely improve the DS voltages. As shown, the minimum voltages are improved to 0.9855, 0.97, 0.9485 p.u for light, nominal and heavy loading, respectively after applying the proposed EMPA. By comparing the different and equal weights as shown in Table 4, the decrease of the first weight reflects less preference, so the power losses are increased from 222.24 to 236.5717 kW with increase percentage of 6.05%. On contrary, the increase of the second weight reflects higher preference so the OVSI is increased from 83.45 to 86.84 with improving of 3.905%.

TABLE 7. Comparisons for the 33-bus DS for each separate loading.

Loading	Items	Open lines	Sum (Pg)	Losses (kW)	Reduction %
Light	Base	33-37	--	47.06	--
	EMPA	10, 28, 33, 34, 36	1114	14.471	69.25
	MPA	8, 13, 28, 33, 36	1114	14.667	68.84
	HSA [29]	7, 10, 14, 28, 32	889.8	17.78	62.22
	FWA [33]	7, 10, 14, 28, 32	860.7	16.22	65.53
	ISCA 35]	7, 10, 14, 28, 31	786.76	16.24	65.49
Nominal	Base	33-37	--	202.66	--
	EMPA	7, 8, 10, 28 & 32	2229	61.257	69.77
	MPA	10, 14, 28, 32 & 33	2179	63.088	68.87
	RGA [29]	7, 9, 12, 27 & 32	1774	74.32	63.33
	GA [29]	7, 10, 28, 32, & 34	1963.3	75.13	62.92
	HSA [29]	4, 7, 10, 28 & 32	1668.4	73.05	63.95
	FF [34]	8, 9, 28, 32 & 33	1773.8	73.95	63.51
	ISCA 35]	7, 9, 14, 28 & 31	1691.2	66.81	67.03
	FWA [33]	7, 11, 14, 28 & 32	1684.1	67.11	66.89
Heavy	Base	33-37	--	575.31	--
	EMPA	7, 12, 28, 32, 35	3566	160.937	72.02
	MPA	8, 28, 33, 34, 36	3566	161.2782	71.96
	HSA [29]	7, 10, 14, 28, 32	2752.9	194.22	66.23
	FWA [33]	7, 10, 14, 28, 32	2752.9	172.97	69.93
	ISCA 35]	7, 9, 14, 28, 31	2981.2	167.96	70.81

TABLE 8. MPA and EMPA results of for 137-bus DS.

	Base	MPA	Proposed EMPA
Open lines	L1AB, L2AB, L69B: L73B, L69A: L73A	10A-11A, 20A-21A, 15A-46A, 57A-58A, 64A-65A, 11B-43B, 12B-13B, 14B-15B, 57B-58B, 27B-65B, 48A-34B, 26B-27B	13A-14A, 11A-43A, 20A-21A, 58A-59A, 27A-65A, 11B-43B, 13B-21B, 12B-13B, 58B-59B, 61B-62B, 33B-34B, 21A-24B,
DGs Bus Locations	--	45A, 61A, 68A, 61B, 66B, 68B	20A, 21A, 27A, 61A, 27B, 61B
DGs Outputs (kW)	--	78, 1701, 625, 1763, 142, 252	185, 455, 14, 1763, 573, 1433
Losses (kW) & % reduction	449.7914	89.757 , (80.05 %)	82.713 , (81.61 %)

TABLE 9. Robustness indices (kW) of MPA and EMPA of 137-bus DS.

Indices	EO [59]	MPA	Proposed EMPA
Best	88.88285	89.75712	82.71356
Medium	109.4142	128.4479	86.77726414
Worst	143.3815178	176.5363	94.37479349
Std	16.483	32.13236	4.767310567

TABLE 10. Results of MPA and EMPA compared to HHO for 83-bus DS.

Ndg	Algorithm	DG Nodes	DG Size (MW)	Power Factor	Configuration	kW Losses
1	HHO [36]	25	2.80	0.95 (lag)	6,12,33,38,41,54,61, 71,82,85,88,89,91	466.56
	MPA	81	2.985	0.95 (lag)	7, 13, 39, 46, 84, 86, 87 89, 90, 91, 92, 93, 96	463.526
	EMPA	61	3	0.95 (lag)	5, 6, 34, 39, 86, 87, 88, 89, 90, 91, 92, 95, 96	410.898
2	HHO [36]	25	2.80	0.95 (lag)	6,12,32,38,41,54,61, 71,82,85,88,89,91	461.22
		44	3.00	0.95 (lag)		
	MPA	84	0.632	0.95 (lag)	39, 43, 55, 64, 85, 87, 88 89, 90, 91, 92, 93, 94	414.581
		56	2.704	0.95 (lag)		
	EMPA	7	3	0.95 (lag)	32, 46, 54, 85, 86, 87, 88, 89, 90, 91, 93, 95, 96	362.43
		47	3	0.95 (lag)		
3	HHO [36]	25	0.75	0.9931 (lag)	6,12,24,33,38,41,54, 61,71,81,85,88,91	443.97
		44	1.70	0.9943 (lag)		
		26	4.80	0.955 (lag)		
	MPA	8	3	0.95 (lag)	11, 13, 41, 72, 84, 85, 89 90, 91, 92, 93, 94, 96	371.132
		35	2.654	0.95 (lag)		
		5	0.322	0.95 (lag)		
	EMPA	84	3	0.95 (lag)	6, 13, 42, 43, 46, 55, 64, 72, 81, 89, 90, 92, 93	325.754
		72	2.628	0.95 (lag)		
		61	3	0.95 (lag)		
4	HHO [36]	25	2.05	0.95 (lag)	6,12,24,31,41,54,61, 71,81,85,88,91,92	434.97
		44	0.30	0.95 (lag)		
		26	3.00	0.95 (lag)		
		45	3.00	0.95 (lag)		
	MPA	81	3	0.95 (lag)	13, 34, 39, 84, 85, 86, 87, 89, 90, 91, 92, 93, 96	336.9709
		7	3	0.95 (lag)		
		10	0.01	0.95 (lag)		
		5	0.085	0.95 (lag)		
	EMPA	36	0.218	0.95 (lag)	7, 34, 62, 76, 83, 84, 86, 87, 89, 90, 92, 93, 95	306.3118
		84	2.467	0.95 (lag)		
		54	3	0.95 (lag)		
		72	2.861	0.95 (lag)		
5	HHO [36]	25	2.05	0.95 (lag)	6,12,24,31,41,54,61, 71,81,85,88,91,92	418.82
		44	0.30	0.95 (lag)		
		26	3.00	0.95 (lag)		
		45	3.00	0.95 (lag)		
		66	3.00	0.95 (lag)		
	MPA	6	0.252	0.95 (lag)	11, 32, 39, 84, 85, 87, 88, 89, 90, 91, 92, 93, 96	327.108
		64	1.414	0.95 (lag)		
		7	2.94	0.95 (lag)		
		23	1.208	0.95 (lag)		
		13	1.911	0.95 (lag)		
	EMPA	20	1.125	0.95 (lag)	6, 14, 20, 34, 39, 41, 55 86, 87, 88, 90, 92, 96	258.512
		83	3	0.95 (lag)		
		72	2.549	0.95 (lag)		
		8	3	0.95 (lag)		
				0.95 (lag)		

3) MPA VERSUS EMPA: ROBUSTNESS COMPARISON

Table 5 tabulates the best, medium, worst, and standard deviation of MPA and EMPA. This table shows the significant improvement of the EMPA performance for both cases studied above. For Case 1, the acquired standard deviation using the EMPA is 6.809 compared to 24.059 for the conventional MPA. In addition, the proposed EMPA achieves lower best of 227.3, medium of 237.81 and worst of 248.18 compared to 246.47, 278.31 and 318.93, for the MPA, respectively. For Case 2, the proposed EMPA records lower standard deviation of 0.0305 than MPA of 0.0879. Additionally, the acquired medium based on EMPA of 1.463 is less than the acquired best based on MPA of 1.467. This affirms the controllability of the new EMPA between discovery and extraction relative to traditional MPA.

4) COMPARATIVE COMPARISON WITH OTHER TECHNIQUES REPORTED CONSIDERING ONE LOADING CONDITION

In order to assess the efficiency of the proposed EMPA on a comparative basis, each load level is considered separately in order to allow comparisons with several other recorded algorithms to handle only a specified loading state, like HSA [29], RGA [29], GA [29], FWA [33], FF [34], SCA [35] and ISCA [35]. By taking one loading stage, the parameters of

TABLE 11. Assessment of the proposed method with those reported in the literature for simultaneous DNR and DGs.

Technique	Merits	Demerits
Ref. [29]	Different loading scenarios	Single objective only and Near optimal solution
[30]	Different patterns of load types	Single objective and Near optimal solution
[33]	Multi-objectives and Different loading scenarios	Near optimal solution and Separate treatment of the loading scenarios
[34]	Multi-objectives, Fixed and dynamic loading	Near optimal solution
[4]	Multi-objectives and Different load types	Peak demand only with Separate treatment of the loading scenarios
[35]	Multi-objectives and Different loading scenarios	Near optimal solution and Separate treatment of the loading scenarios
Proposed Study	1- Multi-objectives 2- Simultaneous treatment of different loading scenarios 3- Validity for real cases studies of Taiwan 83-bus DS. 4- Validity for large scale the 137-bus DS.	

the proposed EMPA are reduced to Maxit = 60, PS = 15. The number of individuals considered is half of the algorithms compared as the proposed EMPA has a double fitness test for each prey. At each loading condition, the MPA and proposed EMPA are both applied in a different manner. Table 6 displays the regarding decision variables, considering light, nominal and heavy loading state. In all cases, the findings indicate the superiority of the new EMPA over the traditional MPA. The proposed EMPA successfully finds smaller value of losses of 14.471, 61.257 and 160.937 kW compared to 14.667, 63.0889, and 161.278 kW for the traditional MPA at light, nominal, and heavy loadings, respectively.

As well, the effects of the MPA and EMPA comparisons with various documented algorithms are summarized in Table 7. This table demonstrates the outperformance of the new EMPA over other prior techniques. In Table 7 (light loading), the proposed EMPA offers the maximum loss reduction of 69.25% while MPA, HSA, FWA and ISCA acquires 68.84, 62.22, 65.53, and 65.49%, respectively. Similarly (nominal loading), the proposed EMPA provides the maximum loss reduction of 69.77% while MPA, RGA, GA, HSA, FWA and ISCA acquires 68.87, 63.33, 62.92, 63.95, 63.51, 67.03, and 66.89%, respectively. Likewise (heavy loading), the proposed EMPA provides the maximum loss reduction of 72.02% while MPA, HSA, FWA and ISCA acquires 71.96, 66.23, 69.93, 70.81%, respectively.

B. OPTIMAL DSR AND DGS INTEGRATION FOR 137-BUS DS

The 137-bus DS is displayed in Fig. 8 [58]. Complete data of the buses loading, and branches resistance and reactance is presented in the Appendix. The proposed EMPA and MPA are employed and applied for DSR and DGs integration for such large-scale DS considering the nominal loading only. Table 8 tabulates the regarding results. As shown, the DS power losses are greatly reduced by 81.16% with the convergence characteristic shown in Fig. 9. Fig. 9 illustrates the good capability of the proposed EMPA in quickly search focusing on the best solution. The statistical results, for this case study, is staggered in Table 9 that explains the higher stability that is become the proposed EMPA compared to MPA and Equilibrium Optimizer (EO) [59] since the proposed EMPA obtains very low standard deviation of 4.76 compared to the traditional MPA of 32.13 and EO of 16.48.

C. OPTIMAL DSR AND DGS INTEGRATION FOR 83-BUS DS

The 83-bus DS is displayed in Fig. 10 [36]. The proposed EMPA and MPA are employed and applied for DSR and DGs integration and compared to recent optimizer of HHO [36]. The comparisons are executed for different number of DGs planning and Table 10 tabulates the obtained nodes, sizes and power factor of the installed DGs with the related configuration based on EMPA, MPA and HHO. From the comparisons in Table 10, the outperformance of the proposed EMPA is very high compared to MPA and HHO [36] for all DGs number considered.

The main merits of applying this work to other DGs planning algorithms in previous works can be summarized as follows:

- Practical load variations are satisfactory covered simultaneously.
- For the 33-bus DS, the proposed EMPA offers the maximum loss reduction compared to HSA [29], RGA [29], GA [29], FF [34], ISCA [35] and FWA [33].
- For the 33-bus DS, the proposed EMPA successfully reduces the cumulative losses by 72.4% compared to 70.36% for MPA for the three-loading process simultaneously.

TABLE 12. Buses and branches data of 137-bus DS.

From	To	kW load	kVar load	R (ohm)	X (ohm)
1A	2A	0	0	0.0005	0.0012
2A	3A	0	0	0.0005	0.0012
3A	4A	0	0	0.0015	0.0036
4A	5A	0	0	0.0251	0.0294
5A	6A	2.6	2.2	0.366	0.1864
6A	7A	40.4	30	0.381	0.1941
7A	8A	75	54	0.0922	0.047
8A	9A	30	22	0.0493	0.0251
9A	10A	28	19	0.819	0.2707
10A	11A	145	104	0.1872	0.0619
11A	12A	145	104	0.7114	0.2351
12A	13A	8	5	1.03	0.34
13A	14A	8	5	1.044	0.34
14A	15A	0	0	1.058	0.3496
15A	16A	45	30	0.1966	0.065
16A	17A	60	35	0.3744	0.1238
17A	18A	60	35	0.0047	0.0016
18A	19A	0	0	0.3276	0.1083
19A	20A	1	0.6	0.2106	0.069
20A	21A	114	81	0.3416	0.1129
21A	22A	5	3.5	0.014	0.0046
22A	23A	0	0	0.1591	0.0526
23A	24A	28	20	0.3463	0.1145
24A	25A	0	0	0.7488	0.2475
25A	26A	14	10	0.3089	0.1021
26A	27A	14	10	0.1732	0.0572
3A	28A	26	18.6	0.0044	0.0108
28A	29A	26	18.6	0.064	0.1565
29A	30A	0	0	0.3978	0.1315
30A	31A	0	0	0.0702	0.0232
31A	32A	0	0	0.351	0.116
32A	33A	14	10	0.839	0.2816
33A	34A	19.5	14	1.708	0.5646
34A	35A	6	4	1.474	0.4873
3A	36A	26	18.6	0.0044	0.0108
36A	37A	26	18.6	0.064	0.1565
37A	38A	0	0	0.1053	0.123
38A	39A	24	17	0.0304	0.0355
39A	40A	24	17	0.0018	0.0021
40A	41A	1.2	1	0.7283	0.8509
41A	42A	0	0	0.31	0.3623
42A	43A	6	4.3	0.041	0.0478
43A	44A	0	0	0.0092	0.0116
44A	45A	39.2	26.3	0.1089	0.1373
45A	46A	39.2	26.3	0.0009	0.0012
4A	47A	0	0	0.0034	0.0084
47A	48A	79	56.4	0.0851	0.2083
48A	49A	384.7	274.5	0.2898	0.7091
49A	50A	384.7	274.5	0.0822	0.2011
8A	51A	40.5	28.3	0.0928	0.0473
51A	52A	3.6	2.7	0.3319	0.114
9A	53A	4.3	3.5	0.174	0.0886
53A	54A	26.4	19	0.203	0.1034
54A	55A	24	17.2	0.2842	0.1447
55A	56A	0	0	0.2813	0.1433
56A	57A	0	0	1.59	0.5337
57A	58A	0	0	0.7837	0.263
58A	59A	100	72	0.3042	0.1006
59A	60A	0	0	0.3861	0.1172
60A	61A	1244	888	0.5075	0.2585
61A	62A	32	23	0.0974	0.0496
62A	63A	0	0	0.145	0.0738
63A	64A	227	162	0.7105	0.3619
64A	65A	59	42	1.041	0.5302
11A	66A	18	13	0.2012	0.0611
66A	67A	18	13	0.0047	0.0014
12A	68A	28	20	0.7394	0.2444
68A	69A	28	20	0.0047	0.0016
1B	2B	0	0	0.0005	0.0012
2B	3B	0	0	0.0005	0.0012
3B	4B	0	0	0.0015	0.0036
4B	5B	0	0	0.0251	0.0294
5B	6B	2.6	2.2	0.366	0.1864
6B	7B	40.4	30	0.381	0.1941
7B	8B	75	54	0.0922	0.047
8B	9B	30	22	0.0493	0.0251
9B	10B	28	19	0.819	0.2707
10B	11B	145	104	0.1872	0.0619
11B	12B	145	104	0.7114	0.2351
12B	13B	8	5	1.03	0.34
13B	14B	8	5	1.044	0.34
14B	15B	0	0	1.058	0.3496
15B	16B	45	30	0.1966	0.065
16B	17B	60	35	0.3744	0.1238
17B	18B	60	35	0.0047	0.0016
18B	19B	0	0	0.3276	0.1083
19B	20B	1	0.6	0.2106	0.069
20B	21B	114	81	0.3416	0.1129
21B	22B	5	3.5	0.014	0.0046
22B	23B	0	0	0.1591	0.0526
23B	24B	28	20	0.3463	0.1145
24B	25B	0	0	0.7488	0.2475
25B	26B	14	10	0.3089	0.1021
26B	27B	14	10	0.1732	0.0572
3B	28B	26	18.6	0.0044	0.0108
28B	29B	26	18.6	0.064	0.1565
29B	30B	0	0	0.3978	0.1315
30B	31B	0	0	0.0702	0.0232
31B	32B	0	0	0.351	0.116
32B	33B	14	10	0.839	0.2816
33B	34B	19.5	14	1.708	0.5646
34B	35B	6	4	1.474	0.4873
3B	36B	26	18.6	0.0044	0.0108
36B	37B	26	18.6	0.064	0.1565
37B	38B	0	0	0.1053	0.123
38B	39B	24	17	0.0304	0.0355
39B	40B	24	17	0.0018	0.0021
40B	41B	1.2	1	0.7283	0.8509
41B	42B	0	0	0.31	0.3623
42B	43B	6	4.3	0.041	0.0478
43B	44B	0	0	0.0092	0.0116
44B	45B	39.2	26.3	0.1089	0.1373
45B	46B	39.2	26.3	0.0009	0.0012
4B	47B	0	0	0.0034	0.0084
47B	48B	79	56.4	0.0851	0.2083
48B	49B	384.7	274.5	0.2898	0.7091
49B	50B	384.7	274.5	0.0822	0.2011
8B	51B	40.5	28.3	0.0928	0.0473
51B	52B	3.6	2.7	0.3319	0.114
9B	53B	4.3	3.5	0.174	0.0886
53B	54B	26.4	19	0.203	0.1034
54B	55B	24	17.2	0.2842	0.1447
55B	56B	0	0	0.2813	0.1433
56B	57B	0	0	1.59	0.5337
57B	58B	0	0	0.7837	0.263
58B	59B	100	72	0.3042	0.1006
59B	60B	0	0	0.3861	0.1172
60B	61B	1244	888	0.5075	0.2585
61B	62B	32	23	0.0974	0.0496
62B	63B	0	0	0.145	0.0738
63B	64B	227	162	0.7105	0.3619
64B	65B	59	42	1.041	0.5302
11B	66B	18	13	0.2012	0.0611
66B	67B	18	13	0.0047	0.0014

- For large-scale 137-bus DS, the proposed EMPA gives the higher stability compared to the traditional MPA and EO [59].
- For 83-bus DS, the proposed EMPA has competitive performance compared with MPA and HHO [36].

TABLE 12. *(Continued.)* **Buses and branches data of 137-bus DS.**

From	To	kW load	kVar load	R (ohm)	X (ohm)
12B	68B	28	20	0.7394	0.2444
68B	69B	28	20	0.0047	0.0016
11A	43A	-	-	0.5	0.5
13A	21A	-	-	0.5	0.5
15A	46A	-	-	1	1
50A	59A	-	-	2	2
27A	65A	-	-	1	1
11B	43B	-	-	0.5	0.5
13B	21B	-	-	0.5	0.5
15B	46B	-	-	1	1
50B	59B	-	-	2	2
27B	65B	-	-	1	1
48A	34B	-	-	0.0002	0.0016
21A	27B	-	-	0.0002	0.0016

V. ASSESSMENT STUDY

Table 11 summarizes the advantages and disadvantages of the competitive techniques compared with EMPA. From this table and previous numerical simulations, it is clear that the EMPA technique has the best solutions for single and multi-objective functions. The main merits of the proposed procedure are:

- Provide a Multiobjective framework
- Validated to small- and large-scale test networks.
- Considering the variation of loading levels.
- Leads to significant techno-economic benefits compared with other competitive techniques.
- High solation quality compared with the reported method.

VI. CONCLUSION

In this paper, an EMPA is presented for simultaneous DSR and DG integration. The suggested EMPA recognizes the scope for differences in environmental and climatic conditions, which show a major change in the MPA standard. Several practical issues are considered; Different loading conditions are concurrently handled; the overall active power losses are reduced while the voltage stability is improved. Technical and operational constraints of voltage quality, current flow through lines, DG penetration restriction and balance equations are maintained. The proposed EMPA is superior compared with the basic MPA and other effective algorithms of GA, RGA, HSA, FF, ISCA, and FWA on the 33-bus distribution network for various separate loading conditions. The proposed EMPA successfully reduces the cumulative losses with 72.4% compared to 70.36% for MPA for the three-loading process at the same time. The proposed EMPA successfully improves the minimum voltage for heavy, nominal and light loading conditions to be 98.3, 97, 95.05%, respectively. The proposed EMPA demonstrates higher robust features than the MPA with small standard deviation. A substantial change has arisen in the MPA using the proposed EMPA by decreasing the average percentage of the infeasible problem variables. The proposed EMPA declares increasing in the percentage of the updated solutions replicating the old ones, and the solutions replicating the global best compared to MPA.

Furthermore, its validity for large scale 137-bus DS is further presented and analyzed compared to MPA for large scale 137-bus DS. The proposed EMPA successfully reduces the losses with 81.16% with small standard deviation of 4.76% for the three-loading process at the same time. On contrary, this research is open to cover other relevant challenges as a future work such as the pre-locations of the remote-control switches, the non-dispatchability mode of DGs, partitioning capability under emergency conditions, and so on. Also, the 83-bus test system has been tested for reasonable assessment between the proposed and previous techniques.

Future studies will be conducted to handle the DSR problem with uncertainties due to renewable DGs and loads, using multi-objective algorithms. In addition, the impact of new technologies such as soft open points will be investigated.

APPENDIX

The 137-bus DS consists of 137 node, 136 lines and 12 lines which are in open status. Its line voltage is 12.66 kV while its apparent demand at the nominal condition is 9.3201 MVA, respectively. Table 12 tabulates the buses loading and branches resistance and reactance is presented in the Appendix. The total apparent power is divided into 7.604 MW as active load and 5.3892 MVAr reactive load.

ACKNOWLEDGMENT

The authors would like to acknowledge the financial support received from Taif University Researchers Supporting Project Number TURSP-2020/86, Taif University, Taif, Saudi Arabia.

REFERENCES

[1] E. E. Elattar, A. M. Shaheen, A. M. El-Sayed, R. A. El-Sehiemy, and A. R. Ginidi, "Optimal operation of automated distribution networks based-MRFO algorithm," *IEEE Access*, vol. 9, pp. 19586–19601, 2021, doi: 10.1109/ACCESS.2021.3053479.

[2] A. M. Elsayed, M. M. Hegab, and S. M. Farrag, "Smart residential load management technique for distribution systems' performance enhancement and consumers' satisfaction achievement," *Int. Trans. Electr. Energy Syst.*, vol. 29, no. 4, p. e2795, Apr. 2019, doi: 10.1002/etep.2795.

[3] A. M. Shaheen and R. A. El-Sehiemy, "Optimal co-ordinated allocation of distributed generation units/capacitor banks/voltage regulators by EGWA," *IEEE Syst. J.*, vol. 15, no. 1, pp. 257–264, Mar. 2020, doi: 10.1109/JSYST.2020.2986647.

[4] U. Rauta and S. Mishra, "An improved Elitist–Jaya algorithm for simultaneous network reconfiguration and DG allocation in power distribution systems," *Renew. Energy Focus*, vol. 30, pp. 92–106, Sep. 2019.

[5] A. Merlin and H. Back, "Search for a minimal-loss operating spanning tree configuration in an urban power distribution system," in *Proc. 5th Power Syst. Comput. Conf. (PSCC)*, no. 1, 1975, pp. 1–18.

[6] A. Abur, "A modified linear programming method for distribution system reconfiguration," *Int. J. Electr. Power Energy Syst.*, vol. 18, no. 7, pp. 469–474, Oct. 1996.

[7] F. V. Gomes, S. Carneiro, J. L. R. Pereira, M. P. Vinagre, P. A. N. Garcia, and L. R. Araujo, "A new heuristic reconfiguration algorithm for large distribution systems," *IEEE Trans. Power Syst.*, vol. 20, no. 3, pp. 1373–1378, Aug. 2005.

[8] A. González, F. M. Echavarren, L. Rouco, and T. Gomez, "A sensitivities computation method for reconfiguration of radial networks," *IEEE Trans. Power Syst.*, vol. 27, no. 3, pp. 1294–1301, Aug. 2012.

[9] H. M. Khodr, J. Martinez-Crespo, M. A. Matos, and J. Pereira, "Distribution systems reconfiguration based on OPF using Benders decomposition," *IEEE Trans. Power Del.*, vol. 24, no. 4, pp. 2166–2176, Oct. 2009.

[10] H. Ahmadi and J. R. Martí, "Linear current flow equations with application to distribution systems reconfiguration," *IEEE Trans. Power Syst.*, vol. 30, no. 4, pp. 2073–2080, Jul. 2015.

[11] Q. Peng, Y. Tang, and S. H. Low, "Feeder reconfiguration in distribution networks based on convex relaxation of OPF," *IEEE Trans. Power Syst.*, vol. 30, no. 4, pp. 1793–1804, Jul. 2015.

[12] T. T. Nguyen and A. V. Truong, "Distribution network reconfiguration for power loss minimization and voltage profile improvement using cuckoo search algorithm," *Int. J. Elect. Power Energy Syst.*, vol. 68, pp. 233–242, Jun. 2015.

[13] H. de Faria, M. G. Resende, and D. Ernst, "A biased random key genetic algorithm applied to the electric distribution network reconfiguration problem," *J. Heuristics*, vol. 23, no. 6, pp. 533–550, 2017.

[14] M. Abdelaziz, "Distribution network reconfiguration using a genetic algorithm with varying population size," *Electr. Power Syst. Res.*, vol. 142, pp. 9–11, Jan. 2017.

[15] A. M. Shaheen and R. A. El-Sehiemy, "Enhanced feeder reconfiguration in primary distribution networks using backtracking search technique," *Austral. J. Elect. Electron. Eng.*, vol. 17, no. 3, pp. 196–202, Sep. 2020.

[16] M. Ettehadi, H. Ghasemi, and S. Vaez-Zadeh, "Voltage stability-based DG placement in distribution networks," *IEEE Trans. Power Del.*, vol. 28, no. 1, pp. 171–178, Jan. 2013.

[17] N. Acharya, P. Mahat, and N. Mithulananthan, "An analytical approach for DG allocation in primary distribution network," *Int. J. Electr. Power Energy Syst.*, vol. 28, no. 10, pp. 669–678, Dec. 2006.

[18] D. Q. Hung, N. Mithulananthan, and R. C. Bansal, "Analytical expressions for DG allocation in primary distribution networks," *IEEE Trans. Energy Convers.*, vol. 25, no. 3, pp. 814–820, Sep. 2010.

[19] I. Quadri, S. Bhowmickr, and D. Joshi, "A multi-objective approach to maximize loadability of distribution networks by simultaneous reconfiguration and allocation of distributed energy resources," *IET Gener., Transmiss. Distrib.*, vol. 12, no. 21, pp. 5700–5712, 2018.

[20] T. H. Khoa, P. Nallagownden, Z. Baharudin, and V. N. Dieu, "One rank cuckoo search algorithm for optimal placement of multiple distributed generators in distribution networks," in *Proc. IEEE Region 10 Conf. (TENCON)*, Nov. 2017, pp. 1715–1720.

[21] T. P. Nguyen and D. N. Vo, "A novel stochastic fractal search algorithm for optimal allocation of distributed generators in radial distribution systems," *Appl. Soft Comput.*, vol. 70, pp. 773–796, Sep. 2018.

[22] A. A. A. El-Ela, R. A. El-Sehiemy, A. M. Shaheen, and I. A. Eissa, "Optimal coordination of static VAR compensators, fixed capacitors, and distributed energy resources in Egyptian distribution networks," *Int. Trans. Electr. Energy Syst.*, vol. 30, no. 11, Sep. 2020, Art. no. e12609.

[23] A. A. A. El-Ela, S. M. Allam, A. M. Shaheen, and N. A. Nagem, "Optimal allocation of biomass distributed generation in distribution systems using equilibrium algorithm," *Int. Trans. Electr. Energy Syst.*, vol. 31, no. 2, Dec. 2020, Art. no. e12727, doi: 10.1002/2050-7038.12727.

[24] S. Das, D. Das, and A. Patra, "Operation of distribution network with optimal placement and sizing of dispatchable DGs and shunt capacitors," *Renew. Sustain. Energy Rev.*, vol. 113, Oct. 2019, Art. no. 109219.

[25] P. D. Huy, V. K. Ramachandaramurthy, J. Y. Yong, K. M. Tan, and J. B. Ekanayake, "Optimal placement, sizing and power factor of distributed generation: A comprehensive study spanning from the planning stage to the operation stage," *Energy*, vol. 195, Mar. 2020, Art. no. 117011.

[26] A. Jafari, H. G. Ganjehlou, T. Khalili, B. Mohammadi-Ivatloo, A. Bidram, and P. Siano, "A two-loop hybrid method for optimal placement and scheduling of switched capacitors in distribution networks," *IEEE Access*, vol. 8, pp. 38892–38906, 2020.

[27] A. Jafari, T. Khalili, E. Babaei, and A. Bidram, "A hybrid optimization technique using exchange market and genetic algorithms," *IEEE Access*, vol. 8, pp. 2417–2427, 2020.

[28] T. Khalili, A. Bidram, and M. J. Reno, "Impact study of demand response program on the resilience of dynamic clustered distribution systems," *IET Gener., Transmiss. Distrib.*, vol. 14, no. 22, pp. 5230–5238, Nov. 2020.

[29] R. S. Rao, K. Ravindra, K. Satish, and S. V. L. Narasimham, "Power loss minimization in distribution system using network reconfiguration in the presence of distributed generation," *IEEE Trans. Power Syst.*, vol. 28, no. 1, pp. 317–325, Feb. 2013.

[30] H. R. Esmaeilian and R. Fadaeinedjad, "Energy loss minimization in distribution systems utilizing an enhanced reconfiguration method integrating distributed generation," *IEEE Syst. J.*, vol. 9, no. 4, pp. 1430–1439, Dec. 2015.

[31] M. M. Aman, G. B. Jasmon, H. Mokhlis, and A. H. A. Bakar, "Optimum tie switches allocation and DG placement based on maximisation of system loadability using discrete artificial bee colony algorithm," *IET Gener., Transmiss. Distrib.*, vol. 10, no. 10, pp. 2277–2284, Jul. 2016.

[32] A. A. A. El-Ela, R. A. El-Sehiemy, A. M. Shaheen, and N. Kotb, "Optimal Allocation of DGs with network reconfiguration using Improved Spotted Hyena Algorithm," *WSEAS Trans. Power Syst.*, vol. 15, pp. 60–67, Apr. 2020.

[33] A. M. Imran, M. Kowsalya, and D. P. Kothari, "A novel integration technique for optimal network reconfiguration and distributed generation placement in power distribution networks," *Int. J. Elect. Power Energy Syst.*, vol. 63, pp. 461–472, Dec. 2014.

[34] O. Badran, H. Mokhlis, S. Mekhilef, W. Dahalan, and J. Jallad, "Minimum switching losses for solving distribution NR problem with distributed generation," *IET Gener., Transmiss. Distrib.*, vol. 12, no. 8, pp. 1790–1801, Apr. 2018.

[35] U. Raut and S. Mishra, "An improved sine–cosine algorithm for simultaneous network reconfiguration and DG allocation in power distribution systems," *Appl. Soft Comput.*, vol. 92, Jul. 2020, Art. no. 106293.

[36] I. M. Diaaeldin, S. H. E. A. Aleem, A. El-Rafei, A. Y. Abdelaziz, and M. Calasan, "Optimal network reconfiguration and distributed generation allocation using Harris hawks optimization," in *Proc. 24th Int. Conf. Inf. Technol. (IT)*, Feb. 2020, pp. 1–6.

[37] I. M. Diaaeldin, S. H. E. A. Aleem, A. El-Rafei, and A. Y. Abdelaziz, "A novel reconfiguration methodology of radial distribution systems for power loss minimization using expanded invasive weed optimization," in *Proc. 21st Int. Middle East Power Syst. Conf. (MEPCON)*, Dec. 2019, pp. 119–124.

[38] A. M. Shaheen and R. A. El-Sehiemy, "A multiobjective salp optimization algorithm for techno-economic-based performance enhancement of distribution networks," *IEEE Syst. J.*, vol. 15, no. 1, pp. 1458–1466, Mar. 2021, doi: 10.1109/JSYST.2020.2964743.

[39] Q. Chen, W. Wang, H. Wang, J. Wu, and J. Wang, "An improved beetle swarm algorithm based on social learning for a game model of multiobjective distribution network reconfiguration," *IEEE Access*, vol. 8, pp. 200932–200952, 2020.

[40] Z. M. Ali, I. M. Diaaeldin, S. H. E. Abdel Aleem, A. El-Rafei, A. Y. Abdelaziz, and F. Jurado, "Scenario-based network reconfiguration and renewable energy resources integration in large-scale distribution systems considering parameters uncertainty," *Mathematics*, vol. 9, no. 1, p. 26, Dec. 2020.

[41] I. M. Diaaeldin, S. H. E. A. Aleem, A. El-Rafei, A. Y. Abdelaziz, and A. F. Zobaa, "A novel graphically-based network reconfiguration for power loss minimization in large distribution systems," *Mathematics*, vol. 7, no. 12, p. 1182, Dec. 2019.

[42] M. B. Shafik, H. Chen, G. I. Rashed, R. A. El-Sehiemy, M. R. Elkadeem, and S. Wang, "Adequate topology for efficient energy resources utilization of active distribution networks equipped with soft open points," *IEEE Access*, vol. 7, pp. 99003–99016, 2019.

[43] A. M. Shaheen, E. E. Elattar, R. A. El-Sehiemy, and A. M. Elsayed, "An improved sunflower optimization algorithm-based Monte Carlo simulation for efficiency improvement of radial distribution systems considering wind power uncertainty," *IEEE Access*, vol. 9, pp. 2332–2344, 2021.

[44] R. Bhugwandeen and A. K. Saha, "Improving reliability on distribution systems by means of network reconfiguration," in *Proc. IEEE PES/IAS PowerAfrica*, Jun. 2018, pp. 220–225.

[45] H. Xing and X. Sun, "Distributed generation locating and sizing in active distribution network considering network reconfiguration," *IEEE Access*, vol. 5, pp. 14768–14774, 2017.

[46] J. Zhu, W. Gu, G. Lou, L. Wang, B. Xu, M. Wu, and W. Sheng, "Learning automata-based methodology for optimal allocation of renewable distributed generation considering network reconfiguration," *IEEE Access*, vol. 5, pp. 14275–14288, 2017.

[47] M. Nick, R. Cherkaoui, and M. Paolone, "Optimal planning of distributed energy storage systems in active distribution networks embedding grid reconfiguration," *IEEE Trans. Power Syst.*, vol. 33, no. 2, pp. 1577–1590, Mar. 2018.

[48] H. M. A. Ahmed and M. M. A. Salama, "Energy management of AC-DC hybrid distribution systems considering network reconfiguration," *IEEE Trans. Power Syst.*, vol. 34, no. 6, pp. 4583–4594, Nov. 2019.
[49] Y. Liu, J. Li, and L. Wu, "Coordinated optimal network reconfiguration and voltage regulator/DER control for unbalanced distribution systems," *IEEE Trans. Smart Grid*, vol. 10, no. 3, pp. 2912–2922, May 2019.
[50] P. Gangwar, A. Mallick, S. Chakrabarti, and S. N. Singh, "Short-term forecasting-based network reconfiguration for unbalanced distribution systems with distributed generators," *IEEE Trans. Ind. Informat.*, vol. 16, no. 7, pp. 4378–4389, Jul. 2020.
[51] J. Wang, W. Wang, Z. Yuan, H. Wang, and J. Wu, "A Chaos disturbed beetle antennae search algorithm for a multiobjective distribution network reconfiguration considering the variation of load and DG," *IEEE Access*, vol. 8, pp. 97392–97407, 2020.
[52] Y. Wang, Y. Xu, J. Li, J. He, and X. Wang, "On the radiality constraints for distribution system restoration and reconfiguration problems," *IEEE Trans. Power Syst.*, vol. 35, no. 4, pp. 3294–3296, Jul. 2020.
[53] M. Usama, M. Moghavvemi, H. Mokhlis, N. N. Mansor, H. Farooq, and A. Pourdaryaei, "Optimal protection coordination scheme for radial distribution network considering ON/OFF-grid," *IEEE Access*, vol. 9, pp. 34921–34937, 2021.
[54] A. M. Shaheen, S. R. Spea, S. M. Farrag, and M. A. Abido, "A review of meta-heuristic algorithms for reactive power planning problem," *Ain Shams Eng. J.*, vol. 9, no. 2, pp. 215–231, Jun. 2018.
[55] A. M. Shaheen, A. M. Elsayed, and M. A. E. Aziz, "Capacitor switching with distribution system reconfiguration and load variations: Practical case study using ETAP and network analyzer," in *Proc. 21st Int. Middle East Power Syst. Conf. (MEPCON)*, Dec. 2019, pp. 562–567.
[56] A. Faramarzi, M. Heidarinejad, S. Mirjalili, and A. H. Gandomi, "Marine predators algorithm: A nature-inspired metaheuristic," *Expert Syst. Appl.*, vol. 152, Aug. 2020, Art. no. 113377.
[57] A. I. Selvakumar and K. Thanushkodi, "A new particle swarm optimization solution to nonconvex economic dispatch problems," *IEEE Trans. Power Syst.*, vol. 22, no. 1, pp. 42–51, Feb. 2007.
[58] E. R. Ramos, A. G. Exposito, J. R. Santos, and F. L. Iborra, "Path-based distribution network modeling: Application to reconfiguration for loss reduction," *IEEE Trans. Power Syst.*, vol. 20, no. 2, pp. 556–564, May 2005.
[59] A. M. Shaheen, A. M. Elsayed, R. A. El-Sehiemy, and A. Y. Abdelaziz, "Equilibrium optimization algorithm for network reconfiguration and distributed generation allocation in power systems," *Appl. Soft Comput.*, vol. 98, Jan. 2021, Art. no. 106867.